Ab initio calculation of ICD widths in photoexcited HeNe

G. Jabbari, S. Klaiman, Y.-C. Chiang, F. Trinter, T. Jahnke, and K. Gokhberg

Citation: The Journal of Chemical Physics **140**, 224305 (2014); doi: 10.1063/1.4881598
View online: http://dx.doi.org/10.1063/1.4881598
View Table of Contents: http://scitation.aip.org/content/aip/journal/jcp/140/22?ver=pdfcov
Published by the AIP Publishing

Ab initio calculation of ICD widths in photoexcited HeNe

G. Jabbari,[1] S. Klaiman,[1] Y.-C. Chiang,[1] F. Trinter,[2] T. Jahnke,[2] and K. Gokhberg[1,a)]
[1]*Theoretische Chemie, Physikalisch-Chemisches Institut, Universität Heidelberg, Im Neuenheimer Feld 229, D-69120 Heidelberg, Germany*
[2]*Institut für Kernphysik, Goethe-Universität Frankfurt, Max-von-Laue-Str. 1, D-60438 Frankfurt, Germany*

(Received 25 March 2014; accepted 23 May 2014; published online 9 June 2014)

Excitation of HeNe by synchrotron light just below the frequency of the $1s \rightarrow 3p$ transition of isolated He has been recently shown to be followed by resonant interatomic Coulombic decay (ICD). The vibrationally resolved widths of the ICD states were extracted with high precision from the photoion spectra. In this paper, we report the results of *ab initio* calculations of these widths. We show that interaction between electronic states at about the equilibrium distance of HeNe makes dark states of He accessible for the photoexcitation and subsequent electronic decay. Moreover, the values of the calculated widths are shown to be strongly sensitive to the presence of the non-adiabatic coupling between the electronic states participating in the decay. Therefore, only by considering the complete manifold of interacting decaying electronic states a good agreement between the measured and computed ICD widths can be achieved. © *2014 AIP Publishing LLC*. [http://dx.doi.org/10.1063/1.4881598]

I. INTRODUCTION

Localized electronic excitations in van der Waals and hydrogen bonded systems have been shown to relax efficiently by the interatomic Coulombic decay (ICD) mechanism.[1] ICD will happen whenever the excess energy of such excitation is higher than the first ionization potential of the neighboring species, thus, the exact process whereby the excited state is produced playing no role. Indeed, ICD has been observed in weakly bound clusters following the absorption of VUV and X-ray photons,[2,3] or the impact of fast electrons[4] and energetic ions.[5–7] Once the energy is locally deposited by a projectile, ICD can either be the only electronic decay process to happen, or it may appear as a part of a more complicated decay cascade. For example, it was shown to accompany both Auger and resonant Auger decay processes taking place in an environment.[8–13]

The decaying ICD state is an example of the Fano-Feshbach resonance and is characterized by a finite lifetime. The knowledge of this lifetime is important for a number of reasons. First, the energy distribution of slow ICD electrons arising from the ionization of the neighboring species depends strongly on it.[14,15] Second, if other relaxation pathways are available for the excited state, such as photon emission or nuclear rearrangement, the corresponding lifetimes define the relative importance of these concurrent processes.[16,17] The major source of information about the ICD lifetimes has been *ab initio* calculations.[3,18] Computed lifetimes were found to be tens to hundreds of femtoseconds in rare gas dimers, while in systems with a large number of neighbors nearest to the excited species (e.g., larger rare gas clusters[19] or endohedral fullerenes[20]) they could be as short as a few femtoseconds. Their quality was mostly assessed only indirectly by employing them in computing ICD electron spectra and comparing the latter with the available experimental results. There were few opportunities for the direct comparison of the *ab initio* and experimental lifetimes due to the dearth of experimental data and complexity of the systems where the measurements had been performed. Indeed, until very recently there were only two direct measurements of ICD lifetimes: in large Ne clusters,[21] and in aqueous solutions of third row metal cations.[22] In both systems, the quantity of interest was inferred from the additional broadening of the photoelectron line due to ICD. The experimental data for Ne clusters agreed within an order of magnitude with the *ab initio* calculations in model Ne clusters.[19]

The ICD lifetimes (or related quantities ICD widths) in a certain excited electronic state depend strongly on the vibrational state populated in the transition. However, a measurement in larger systems results in averaging over an ensemble obscuring finer details of the interatomic decay and complicating the comparison with the computed lifetimes. Much better insight into the dynamics of ICD was allowed by two recent time-resolved experiments with rare gas dimers. In the first experiment, Trinter *et al.*[23] utilized the post collision interaction (PCI) effect to observe the temporal evolution of ICD following ionization of the He dimer. The term post collision interaction refers to the phenomenon of energy exchange between the slow primary electron and the fast secondary electron studied primarily for the Auger decay process (see, e.g., Refs. 24 and 25). The magnitude of this exchange sensitively depends on the exact moment the decay happens. Coincident measurement of the slow photoelectron carrying the decay's time stamp and the kinetic energy release of the He nuclei following the ICD event allowed to reconstruct the progression of ICD with time. No experimental lifetimes were reported; however, the experimental survival probability of the decaying state was shown to agree reasonably well with the theoretical result and to exhibit non-exponential behavior. Furthermore, the evolution of the kinetic energy release, i.e., the nuclear dynamics during the decay, agreed nicely with theoretical predictions.[15,23,26]

a)Electronic mail: kirill@pci.uni-heidelberg.de

In the second experiment, Schnorr *et al.*[27] studied the temporal evolution of ICD in Ne_2 following the ionization of an inner-valence 2*s* electron by using the pump-probe technique. They were able to unambiguously identify the ions produced in ICD and measure their yield as a function of the pump-probe delay time. Although the decay showed a non-exponential character, by approximating the yield function through a single exponential curve they estimated the corresponding lifetime to be 150 ± 50 fs which accorded fairly well with the *ab initio* results of about 60 fs[28] and 90 fs.[29]

The non-exponential behavior of the survival probability, even in such small systems as the He and Ne dimers, is due primarily to the presence of several decaying vibrational states each characterized by a specific lifetime. The occupation of several states in the excitation step leads to temporal evolution of the nuclear wavepacket on the excited potential energy curve. During this nuclear dynamics each of the vibrational states decays with its own rate resulting in the non-exponential survival probability. This is indeed the case under the conditions of the experiments described above, where the ICD state is created in a photoionization event and either ICD electron or both ICD and photo-electron are not observed. If, on the contrary, one populates a single vibrational state in the electronically excited state which undergoes ICD, then the observed temporal evolution of the ICD process should be exponential and, thus, characterized by a well defined lifetime. Such individual ICD states can be accessed more easily if they are prepared through resonant photoabsorption.

In a recent publication, we demonstrated ICD from individual vibronic levels of the resonantly excited HeNe dimer.[30] We will give a brief outline of the experiment and refer the reader to the original publication for the details. The HeNe dimer was irradiated by synchrotron light with a photon energy about 23.087 eV which corresponds to the energy of the dipole-allowed excited $1s3p\ ^1P^0$ state of isolated He. Absorption of such photon leads to the ionization of HeNe resulting in $HeNe^+$ cations which were observed in the experiment. This ionization may proceed non-resonantly, with an electron being directly removed from Ne. Alternatively, the photon can be resonantly absorbed by the He atom, which then de-excites by transferring the excess energy to and ionizing the Ne atom. In a recent work, Müller and Voitkiv[31] demonstrated the importance of this ICD process for the enhancement of photoionization. Specifically, they showed that whenever the conditions for the resonant absorption are fulfilled, the interatomic decay leads to a dramatic enhancement in the ionization of the neighbor. This was indeed observed in the experiment where the production of $HeNe^+$ was enhanced about hundred-fold close to the resonant frequency of He. Moreover, scanning below the atomic frequency revealed that the photoionization peak is a vibrational progression. Each term in these series was broadened with the width exceeding the natural linewidth of the synchrotron beam, 1.7 meV. The additional broadening was attributed to ICD and the corresponding lifetimes of the vibrational states were extracted from the spectrum.

These experimental lifetimes give us a rare opportunity for a detailed comparison of the theoretical calculations with the results of an experiment. In this article, we discuss in detail the *ab initio* calculations of the ICD lifetimes of the HeNe states originating from the $He(1s3p\ ^1P^0)$ state. We demonstrate that the observed lifetimes depend sensitively on the structure of and interactions in the manifold of electronic states. In particular, we show that the inclusion of the non-adiabatic coupling in the calculations improves the correspondence between the measured and calculated ICD lifetimes.

II. COMPUTATIONAL DETAILS

The quantities obtained in the experiment were the positions, ICD widths, and intensities of the lines in the photoion yield spectrum of HeNe. To obtain these quantities theoretically, one needs first to compute the complex potential energy curves (PECs) with the imaginary part corresponding to the purely electronic ICD width and electronic dipole transition moments. These, in turn, are used to solve the Schrödinger equation for the nuclear motion producing the full meta-stable vibrational spectrum.

The experiment was carried out at a very high photon energy resolution so that decaying states differing by only a few meV in energies could be separated in the spectrum. Therefore, the *ab initio* real part of the PECs should be obtained in similar precision to allow for a meaningful assignment of the decaying vibrational states. We have seen that the PECs obtained on the EOM-CCSD level tended to underestimate the binding energies which resulted in noticeable overestimation of the excitation energies of the lowest terms in the measured progression. We could achieve acceptable agreement with the experiment in the positions of the peaks only by computing the adiabatic PECs of the excited states on the CR-EOMCC(2,3) level. To this end, we used the implementation of the method included in the GAMESS-US program suite.[32–34] The adiabatic dipole transition moments were computed on the EOM-CCSD level using the MOLPRO program suite.[35–37] The ground state PEC was computed on the CCSD(T) level using the MOLPRO program suite and the resulting PEC was corrected for the basis set superposition error. We found that the dimer was bound in its electronic ground state by 1.55 meV, with the equilibrium distance R_{eq} = 3.065 Å. The data are in good agreement with the accurate calculations of Ref. 38 (D_e = 1.8 meV, R_{eq} = 3.035 Å).

We used the cc-pV5Z basis set[39] augmented by 4 *s*-type, 5 *p*-type, 5 *d*-type even-tempered Gaussian type orbitals (β = 2.5) on He. For this basis set, the energies of the $1s \rightarrow 3p\ ^1P^0$ and $1s \rightarrow 3d\ ^1D$ transitions in He were found at 23.079 eV and 23.067 eV as compared to the experimental values of 23.087 eV and 23.074 eV.[40] In the HeNe dimer, these states are embedded into the electronic continuum corresponding to the $HeNe^+$ target. Therefore, in selecting the basis set for Ne we had to keep in mind that what we actually tried to compute was the approximate real part of a resonance potential energy surface. This could be done, since, due to the incompleteness of the basis sets, the diagonalization of the *ab initio* electronic Hamiltonian resulted not in a true electronic continuum but in a discretized pseudo-continuum allowing one to identify the resonance state of interest. Increasing the basis set on Ne led on the one hand to the improvement in the interaction energy in the excited states of the dimer. On

the other hand, it increased the density of the pseudo-continuum in the energy range of interest making the identification of the resonance curve more difficult. We would also like to note that by keeping the pseudo-continuum sparse one neglects the shift of the real part of the resonance energy due to the interaction with the continuum. This imposes a natural limitation on the accuracy of the PECs we can achieve. This shift in the ICD region can reach a few meV. Therefore, the aug-cc-pV5Z basis set[41] we chose for Ne offered an optimal solution in terms of accuracy and computational effort.

The adiabatic electronic ICD widths Γ(R), representing the imaginary parts of the corresponding PECs, were computed by the ADC-Fano-Stieltjes method.[42] We used the cc-pV5Z basis set augmented by 4 *s*-type, 5 *p*-type, 5 *d*-type even-tempered Gaussian type orbitals ($\beta = 2.5$) on He, and the cc-pV5Z basis set augmented by 4 *s*-type, 4 *p*-type, 4 *d*-type even-tempered Gaussian type orbitals ($\beta = 2.5$) on Ne. The final states (P-space) were constructed by using all singly and doubly excited intermediate states with one and, respectively, two holes localized on the Ne atom. The decaying state was constructed by using all singly and doubly excited intermediate states with at least one hole localized on the He atom.

The energies and ICD widths of the vibrational levels in the excited adiabatic electronic states in question were obtained by diagonalizing a non-hermitian adiabatic Hamiltonian, given below in the local approximation[43] as

$$\hat{H}_d = \hat{T}_N + V(R) - \frac{i}{2}\Gamma(R), \tag{1}$$

where V(R) is the real part of an adiabatic resonance PEC and Γ(R) is the electronic ICD width. To diagonalize the Hamiltonian, we represented it in the region 1.51 Å ≤ R ≤ 21.96 Å on a grid of 2046 points using the discrete variable representation (sine-DVR) method.[44]

To estimate the effect of the non-adiabatic coupling between the adiabatic PECs of the He($1s \rightarrow 3p\pi$)Ne and He($1s \rightarrow 3d\pi$)Ne states on the decay widths it is easier to work in the so called diabatic representation. We obtained the diabatic PECs, $W_{1,2}$(R), from the adiabatic ones under the assumption that the vibronic coupling, Δ, was constant (see, e.g., Ref. 45). The approximately diabatic decay widths Γ′(R) and dipole transition moments were obtained by interconnecting smoothly the adiabatic quantities on both sides of the discontinuities arising due to the avoided crossing (see Figs. 1 and 2). The energies and widths of the vibronic states were obtained by diagonalizing the Hamiltonian of the coupled diabatic states

$$\hat{H}'_d = \begin{pmatrix} \hat{T}_N + W_1(R) - \frac{i}{2}\Gamma'_1(R) & \Delta \\ \Delta & \hat{T}_N + W_2(R) - \frac{i}{2}\Gamma'_2(R) \end{pmatrix}, \tag{2}$$

where the indices denote the coupled electronic states. We found that the vibronic coupling in our case was equal to 0.54 meV, an order of magnitude larger than the decay widths at the position of the avoided crossing. We could, therefore, neglect in Eq. (2) the coupling between the surfaces proceeding via electronic continuum.[46] The Hamiltonian in Eq. (2) was diagonalized using the same grid and DVR as in the previous case.

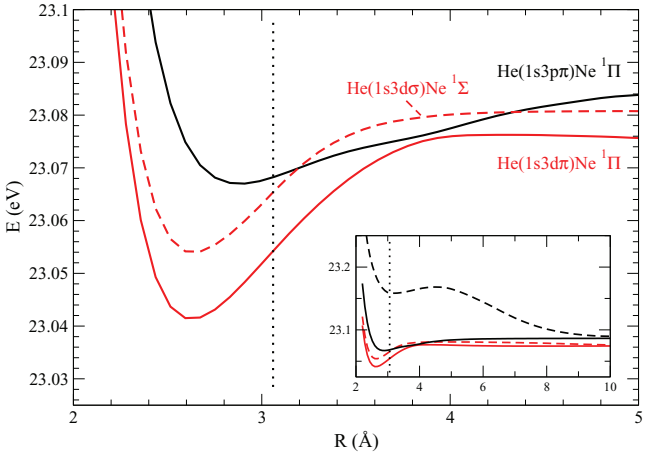

FIG. 1. Adiabatic potential energy curves of the HeNe states accessible in photoexcitation about 23.087 eV, the energy of the $1s \rightarrow 3p$ transition in isolated He. The lower solid and broken curves correspond asymptotically to the He($1s3d\pi$)Ne and He($1s3d\sigma$)Ne states. The upper solid and broken (shown only in the inset) curves correspond to the He($1s3p\pi$)Ne and He($1s3p\sigma$)Ne states. The pairs of states in each molecular symmetry interact with each other (see also Figs. 2 and 3). In the Π symmetry, this interaction is visible as the avoided crossing at 3.85 Å, i.e., in the Frank-Condon region. In the Σ symmetry, the curves interact between 5 Å and 8 Å leading to the splitting off of the He($1s3p\sigma$)Ne PEC. The vertical dotted lines in the graph and the inset indicate the ground state equilibrium distance of the neutral HeNe.

III. RESULTS AND DISCUSSION

Photoionization enhancement of weakly bound clusters was experimentally observed at light frequencies close to a resonant frequency of some isolated constituent (see, e.g., Refs. 47–49). This enhancement can be understood in terms of an antenna-receiver picture.[30] At a suitable frequency,

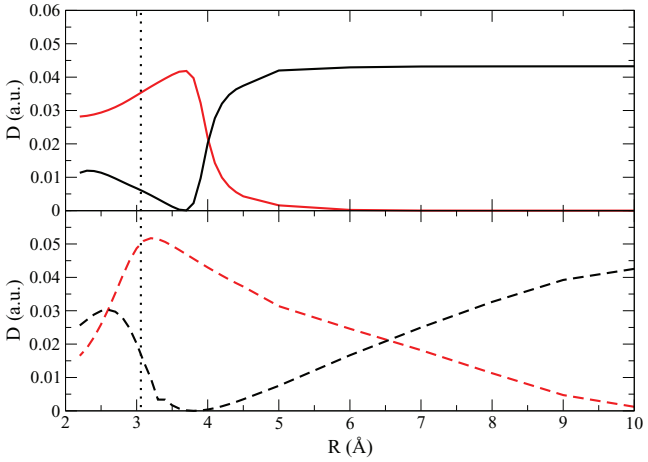

FIG. 2. Adiabatic dipole transition moments to the states of HeNe accessible in photoexcitation about 23.087 eV. (Upper panel) The dipole transition moments to the He($1s3d\pi$)Ne (solid red line) and He($1s3p\pi$)Ne (solid black line) states. Note the discontinuity at about 3.85 Å corresponding to the avoided crossing in the respective PECs. (Lower panel) The dipole transition moments to the He($1s3d\sigma$)Ne (dashed red line) and He($1s3p\sigma$)Ne (dashed black line) states. The vertical dotted line in the graph indicates the ground state equilibrium distance of the neutral HeNe.

the photon is resonantly absorbed by one constituent (antenna); the energy is efficiently transferred by the ICD mechanism to a neighbor (receiver) leading to its ionization.[50] The enhancement is due to the higher probability of a dipole transition between two bound (or more precisely a bound and a quasi-bound) electronic states than that of the direct transition in the electronic continuum.

The lowest energy at which this enhancement may occur in the HeNe dimer is about 23.087 eV. This is the energy of the first dipole allowed excited state of He, He($1s3p\ ^1P^0$), whose energy lies above the lowest ionization potential, 21.56 eV, of Ne. Immediately below this state lies another excited state of He, He($1s3d\ ^1D$), which is quadrupole allowed, and whose excitation in HeNe apparently should not lead to a pronounced photoionization enhancement. However, since asymptotically the difference between the states is only 13 meV, we cannot rule beforehand that at shorter interatomic distances the mixing between the two states would not lead to a sharing of the dipole strength.

We plot in Fig. 1 the adiabatic PECs of the He($1s3p$)Ne and He($1s3d$)Ne states in Σ and Π molecular symmetries. The interaction between the states of Σ symmetry becomes visible already at about 8 Å and leads to the splitting off of the He($1s3p\sigma$)Ne state. The interaction between the states of Π symmetry is noticeably weaker and results in the avoided crossing at 3.85 Å. The differing strength of interaction in these symmetries is due to the different distribution of the densities of the excited electron. In Σ symmetry, the electron occupies either the $3d_{z^2}$ or $3p_z$ virtual orbital, which are aligned along the z-axis and, therefore, strongly perturbed by the Ne atom. The orbitals occupied in Π symmetry are $3d_{xz}$ and $3p_x$ ($3d_{yz}$ and $3p_y$) where the electron density is to a large degree located off the z-axis. The three PECs accessible by photons with energy about 23.087 eV, i.e., He($1s3d\pi$)Ne, He($1s3p\pi$)Ne, and He($1s3d\sigma$)Ne, are all bound and support two, four, and two vibrational states, respectively.

The photoabsorption efficiency of these states is given by the respective dipole transition moments. The adiabatic dipole transition moments are plotted in Fig. 2. One can see from the plot that at large interatomic distances the excitations to the *d*-orbitals carry much less dipole strength than the excitations to the *p*-orbitals. There is a rapid change in the transition moments about the distances where the avoided crossings occur, due to the change in the electronic character of the excited states. Interestingly, this change is abrupt for the states of Π symmetry and gradual for the states of Σ symmetry indicating again in the latter case the extended range over which the interaction is strong. At about the ground state equilibrium interatomic distance the electronic transition dipole moments of all three PECs of interest are non-negligible and the excitation to all three of them should contribute to the photoionization yield.

These excited states lie in and interact with the electronic continuum corresponding to $HeNe^+$. Therefore, these states acquire a width which is inversely proportional to their lifetimes. The adiabatic electronic ICD widths Γ(R) are shown in Fig. 3. One can immediately see that at large interatomic distances the decay widths of the dipole allowed states are 1-2 orders of magnitude larger than the ones of the quadrupole

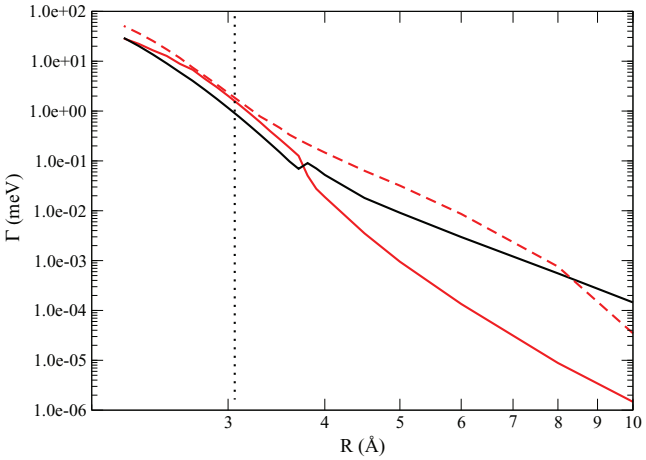

FIG. 3. Adiabatic electronic decay widths of the states of HeNe accessible in photoexcitation about 23.087 eV: He($1s3d\pi$)Ne (solid red line), He($1s3p\pi$)Ne (solid black line), and He($1s3p\sigma$)Ne (broken red line). Note the discontinuity in the widths of the He($1s3d\pi$)Ne and He($1s3p\pi$)Ne states corresponding to the avoided crossing at 3.85 Å. The vertical dotted line in the graph indicates the ground state equilibrium distance of the neutral HeNe.

allowed states. This is in line with the expected asymptotic behavior of these widths which should fall as $1/R^6$ and $1/R^8$, respectively.[42] The width of the He($1s3d\sigma$)Ne state is more than an order of magnitude larger than the width of the He($1s3d\pi$)Ne state; it is mostly due to the already mentioned strong mixing between the dipole and quadrupole allowed states in the Σ symmetry. In the Π symmetry, the widths, like the transition moments, exhibit a sudden jump at the distance corresponding to the avoided crossing. It is important to keep in mind, that the R-dependent electronic ICD width is not an experimentally observable quantity. The observed ICD rate is a function of the decay rates of the occupied vibrational states from which the ICD process initiates. However, if the decay proceeds from an isolated electronic state the value of Γ(R) at the ground state equilibrium distance R_{eq} might serve as a useful estimate of the observable decay width or lifetime. The quality of such an estimate is based on three assumptions: nearly symmetric distribution about R_{eq} of the initial vibrational wavepacket, vertical transition to the excited state, and electronic decay much faster than nuclear dynamics in the excited state. Larger deviations from this lifetime are usually interpreted as an evidence of nuclear dynamics in the decaying state (see, e.g., Ref. 12). The respective widths of the He($1s3d\pi$)Ne, He($1s3p\pi$)Ne, and He($1s3d\sigma$)Ne states at R_{eq} = 3.065 Å are 1.7 meV, 1.35 meV, and 1.9 meV.

Under the conditions of the experiment one could selectively populate individual vibrational states corresponding to the excited electronic states of HeNe, and extract the corresponding ICD widths. The positions, widths, and intensities of the six peaks identified in the experiment are shown in Tables I and II. To assign these peaks, we first diagonalized Eq. (1) independently for the three states in question using the adiabatic PECs and widths. The R-dependent electronic decay width appears as a purely imaginary potential in the nuclear Hamiltonian. As the result, the energies of the vibrational states obtained in the diagonalization acquire constant imaginary parts, $-i\Gamma_n/2$, where Γ_n is the ICD width measured

TABLE I. Positions and interatomic decay widths of the vibrational states supported by the He($1s3d\pi$)Ne, He($1s3p\pi$)Ne, and He($1s3p\sigma$)Ne PECs. The experimental values[30] are compared with the results of *ab initio* calculations in the adiabatic approximation. The adiabatic PECs in the assignment are labelled according to the excited state of He they correlate with asymptotically.

	Experiment			Theory (adiabatic)			
Peak	Energy (eV)	Width (meV)	Intensity	Assignment	Energy (eV)	Width (meV)	Intensity
1	23.0460	5.0 ± 1.5	5%	$1s3d\pi$ v=0	23.0508	3.74	7.7%
2	23.0617	4.5 ± 1.0	13%	$1s3d\sigma$ v=0	23.0633	5.68	7.2%
3	23.0690	3.0 ± 1.0	10%	$1s3d\pi$ v=1	23.0656	2.90	17.3%
4	23.0746	4.0 ± 1.5	38%	$1s3p\pi$ v=0	23.0722	1.41	0.9%
				$1s3d\sigma$ v=1	23.0768	3.66	23.3%
				$1s3p\pi$ v=1	23.0788	0.85	4.4%
5	23.0806	2.5 ± 1.2	30%	$1s3p\pi$ v=2	23.0835	0.62	26.6%
6	23.0851	$0.6^{+1.5}_{-0.3}$	4%	$1s3p\pi$ v=3	23.0859	0.22	12.6%

in the experiment. The vibrational eigenfunctions were used together with the electronic transition moments to obtain the peaks intensities. The results of the adiabatic calculations are shown in Table I.

We found eight bound vibrational states which are supported by the three electronic PECs in question. Comparing the theoretical and experimental results we can unambiguously assign the lowest and two highest lines in the experimental spectrum. The position errors lie between 1 meV and 5 meV in agreement with the expected errors in the electronic PECs. The assignment of the lines in the middle of the spectrum is more tentative. We think that the overlapping peaks corresponding to the He($1s3p\pi$)Ne, $v = 0$, He($1s3p\pi$)Ne, $v = 1$, and He($1s3d\sigma$)Ne, $v = 1$ states are not resolved in the experiment and appear as a single broad peak at 23.0746 eV. Although the peaks corresponding to the He($1s3d\sigma$)Ne, $v = 0$ and He($1s3d\pi$), $v = 1$ states are also not resolved well in our calculation, we assign them to the second and third peaks in the experimental spectrum. The correspondence of the *ab initio* relative line intensities to the experimental ones is acceptable.

Of particular importance to us is the agreement in the computed and measured decay widths. Thus, the numerical widths of the three lowest peaks correspond closely to the experimental results. However, the *ab initio* widths of the two uppermost states are considerably underestimated. Both states belong to the He($1s3p\pi$)Ne adiabatic electronic potential and lie above the avoided crossing with the He($1s3d\pi$)Ne state. The two curves are split by just 0.5 meV at this point and, therefore, the non-adiabatic coupling may become important. If it is taken into account, the energies and widths of the vibrational states should be determined by solving a coupled system of equations (see Eq. (2)). In addition, the He($1s3p\pi$)Ne, v = 1-3 states lie above the dissociation threshold of the He($1s3d\pi$)Ne electronic state. Therefore, the non-adiabatic coupling will cause the former to predissociate, which, in turn, should lead to an additional broadening of the vibrational lines. However, our calculations showed that the effect of this mechanism on the line widths is negligible.

The results of the calculations including the non-adiabatic coupling are given in Table II. By comparing these results with the results of the adiabatic calculation we see that the lower lying states in the Π symmetry remain unaffected. This is not surprising, since the corresponding vibrational wave functions are small at the distance corresponding to the avoided crossing. However, the energies and widths of the higher lying vibrational states in the He($1s3p\pi$)Ne PEC are affected. The coupling of the complex potentials leads to the admixture of the adiabatic width of the He($1s3p\pi$)Ne electronic state to the one of the He($1s3d\pi$)Ne state. Since the electronic decay happens predominantly at shorter interatomic distances where the former width is the larger, the coupling tends to increase the widths of the vibrational v = 1–3 states in the He($1s3p\pi$)Ne PEC. Moreover, the energies of

TABLE II. Positions and interatomic decay widths of the vibrational states supported by the He($1s3d\pi$)Ne, He($1s3p\pi$)Ne, and He($1s3p\sigma$)Ne PECs. The experimental values[30] are compared with the results of *ab initio* calculations where the effects of the non-adiabatic coupling between the PECs of Π symmetry were taken into account. The states of the Σ symmetry are marked by *.

	Experiment			Theory (non-adiabatic)		
Peak	Energy (eV)	Width (meV)	Intensity	Energy (eV)	Width (meV)	Intensity
1	23.0460	5.0 ± 1.5	5%	23.0506	3.74	6.4%
2	23.0617	4.5 ± 1.0	13%	23.0633*	5.68	6.0%
3	23.0690	3.0 ± 1.0	10%	23.0655	2.90	15.0%
4	23.0746	4.0 ± 1.5	38%	23.0722	1.32	0.5%
				23.0759	1.8	21.6%
				23.0768*	3.66	19.4%
5	23.0806	2.5 ± 1.2	30%	23.0823	1.0	18.7%
6	23.0851	$0.6^{+1.5}_{-0.3}$	4%	23.0855	0.42	12.4%

these three states are shifted downwards. The change in the positions and intensities of the lines due to the non-adiabatic interaction does not invalidate the assignment of the lines. Thus, the state $v = 1$ in the He($1s3p\pi$)Ne PEC, whose energy, width, and intensity are changed the most, still overlaps strongly with the He($1s3d\sigma$)Ne $v = 1$ state and can be identified as the broad peak at 23.0746 eV in the experimental spectrum. The corrected He($1s3p\pi$)Ne, $v = 2$–3 states still correspond clearly to the two highest lines in the experimental spectrum. However, one can see that both their positions and, more importantly, widths agree much better with the experimental results.

IV. CONCLUSIONS

In this paper, we presented the results of a calculation of the vibrationally resolved ICD widths for the excited states of the HeNe dimer. These quantities allow for the easiest natural comparison between the results of the theoretical modelling of the decay and the experimental measurements. As we have demonstrated the *ab initio* widths obtained for the excitations of HeNe around the energy of the $1s3p\ ^1P^0$ excitation of isolated He are in excellent agreement with the experimental results. This is the first time the theoretical ICD widths of individual vibrational levels could be compared to their experimental counterparts directly, and not through the medium of other measured quantities, such as electron spectra or kinetic energy release of the nuclei. Moreover, the possibility of such comparison allowed us to investigate in detail how a measured width can be reconstructed theoretically.

There are two important conclusions to be drawn from this investigation. First, it has been customary to think of ICD as proceeding on two separate subsystems, one of which is used to absorb energy from an external agency while another receives the energy from the first subsystem and is ionized. If we apply this thinking to the HeNe problem, then only the states correlating with the dipole allowed excited states of the He atom should be observed in the decay. However, as we have shown the dark, $1s \rightarrow 3d$, states of He mix with and borrow intensity from the bright $1s \rightarrow 3p$ states in the Franck-Condon region of HeNe. Consequently, they will be excited in photoabsorption and decay by ICD. Interestingly, their intensities in the spectra are made even more pronounced by a favorable overlap with the vibrational wave function in the electronic ground state.

The second observation is that the non-adiabatic coupling between the decaying PECs not only changes the nuclear dynamics during the decay, it also changes the magnitude of the decay width for some of the vibrational states. In the HeNe case taking into account this coupling between the states of Π symmetry changed the width of the uppermost states by almost a factor of two and brought them into a much better agreement with the experiment. The influence of the non-adiabatic coupling on the ICD widths was previously discussed by Sisourat *et al.*[15] They demonstrated that the computed ICD yield following photoionization of the He dimer grew significantly when the coupling between close lying PECs of the decaying states was included in the calculations. Therefore, at higher excitation energies, where the density of ICD states is large, the presence of the non-adiabatic interactions may significantly influence the ICD lifetimes.

ACKNOWLEDGMENTS

The work was supported by Research Unit 1789 (Interatomic Coulombic decay) of the Deutsche Forschungsgemeinschaft (DFG). G.J. gratefully acknowledges the financial support of the IMPRS at the MPIK, Heidelberg.

[1] L. S. Cederbaum, J. Zobeley, and F. Tarantelli, Phys. Rev. Lett. **79**, 4778 (1997).
[2] U. Hergenhahn, J. Electron Spectrosc. Relat. Phenom. **184**, 78 (2011).
[3] V. Averbukh, P. V. Demekhin, P. Kolorenč, S. Scheit, S. D. Stoychev, A. I. Kuleff, Y.-C. Chiang, K. Gokhberg, S. Kopelke, N. Sisourat *et al.*, J. Electron Spectrosc. Relat. Phenom. **183**, 36 (2011).
[4] S. Yan, P. Zhang, X. Ma, S. Xu, B. Li, X. L. Zhu, W. T. Feng, S. F. Zhang, D. M. Zhao, R. Zhang *et al.*, Phys. Rev. A **88**, 042712 (2013).
[5] J. Titze, M. Schöffler, H. K. Kim, F. Trinter, M. Waitz, J. Voigtsberger, N. Neumann, B. Ulrich, K. Kreidi, R. Wallauer *et al.*, Phys. Rev. Lett. **106**, 033201 (2011).
[6] H. K. Kim, J. Titze, M. Schöffler, F. Trinter, M. Waitz, J. Voigtsberger, H. Sann, M. Meckel, C. Stuck, U. Lenz *et al.*, Proc. Natl. Acad. Sci. U.S.A. **108**, 11821 (2011).
[7] H. K. Kim, H. Gassert, M. S. Schöffler, J. N. Titze, M. Waitz, J. Voigtsberger, F. Trinter, J. Becht, A. Kalinin, N. Neumann *et al.*, Phys. Rev. A **88**, 042707 (2013).
[8] R. Santra and L. S. Cederbaum, Phys. Rev. Lett. **90**, 153401 (2003).
[9] Y. Morishita, X.-J. Liu, N. Saito, T. Lischke, M. Kato, G. Prümper, M. Oura, H. Yamaoka, Y. Tamenori, I. H. Suzuki *et al.*, Phys. Rev. Lett. **96**, 243402 (2006).
[10] K. Gokhberg, P. Kolorenč, A. I. Kuleff, and L. S. Cederbaum, Nature (London) **505**, 661 (2014).
[11] F. Trinter, M. S. Schöffler, H. K. Kim, F. P. Sturm, K. Cole, N. Neumann, A. Vredenborg, J. Williams, I. Bocharova, R. Guillemin *et al.*, Nature (London) **505**, 664 (2014).
[12] K. Kimura, H. Fukuzawa, T. Tachibana, Y. Ito, S. Mondal, M. Okunishi, M. Schöffler, J. Williams, Y. Jiang, Y. Tamenori *et al.*, J. Phys. Chem. Lett. **4**, 1838 (2013).
[13] P. O'Keeffe, E. Ripani, P. Bolognesi, M. Coreno, M. Devetta, C. Callegari, M. Di Fraia, K. C. Prince, R. Richter, M. Alagia *et al.*, J. Phys. Chem. Lett. **4**, 1797 (2013).
[14] T. Ouchi, K. Sakai, H. Fukuzawa, I. Higuchi, P. V. Demekhin, Y.-C. Chiang, S. D. Stoychev, A. I. Kuleff, T. Mazza, M. Schöffler *et al.*, Phys. Rev. A **83**, 053415 (2011).
[15] N. Sisourat, N. V. Kryzhevoi, P. Kolorenč, S. Scheit, and L. S. Cederbaum, Phys. Rev. A **82**, 053401 (2010).
[16] S. Kopelke, Y. C. Chiang, K. Gokhberg, and L. S. Cederbaum, J. Chem. Phys. **137**, 034302 (2012).
[17] T. Jahnke, H. Sann, T. Havermeier, K. Kreidi, C. Stuck, M. Meckel, M. Schoffler, N. Neumann, R. Wallauer, S. Voss *et al.*, Nature Phys. **6**, 139 (2010).
[18] R. Santra and L. S. Cederbaum, Phys. Rep. **368**, 1 (2002).
[19] R. Santra, J. Zobeley, and L. S. Cederbaum, Phys. Rev. B **64**, 245104 (2001).
[20] V. Averbukh and L. S. Cederbaum, Phys. Rev. Lett. **96**, 053401 (2006).
[21] G. Öhrwall, M. Tschaplyguine, M. Lundwall, R. Feifel, H. Bergersen, T. Rander, A. Lindblad, J. Schulz, S. Peredkov, S. Barth *et al.*, Phys. Rev. Lett. **93**, 173401 (2004).
[22] G. Öhrwall, N. Ottosson, W. Pokapanich, S. Legendre, S. Svensson, and O. Björneholm, J. Phys. Chem. B **114**, 17057 (2010).
[23] F. Trinter, J. B. Williams, M. Weller, M. Waitz, M. Pitzer, J. Voigtsberger, C. Schober, G. Kastirke, C. Müller, C. Goihl *et al.*, Phys. Rev. Lett. **111**, 093401 (2013).
[24] A. Russek and W. Mehlhorn, J. Phys. B **19**, 911 (1986).
[25] S. N. Pisharody and R. R. Jones, Phys. Rev. Lett. **91**, 203002 (2003).
[26] N. Sisourat, N. V. Kryzhevoi, P. Kolorenč, S. Scheit, T. Jahnke, and L. S. Cederbaum, Nature Phys. **6**, 508 (2010).
[27] K. Schnorr, A. Senftleben, M. Kurka, A. Rudenko, L. Foucar, G. Schmid, A. Broska, T. Pfeifer, K. Meyer, D. Anielski *et al.*, Phys. Rev. Lett. **111**, 093402 (2013).

[28]V. Averbukh and L. S. Cederbaum, J. Chem. Phys. **125**, 094107 (2006).
[29]N. Vaval and L. S. Cederbaum, J. Chem. Phys. **126**, 164110 (2007).
[30]F. Trinter, J. B. Williams, M. Weller, M. Waitz, M. Pitzer, J. Voigtsberger, C. Schober, G. Kastirke, C. Müller, C. Goihl *et al.*, Phys. Rev. Lett. **111**, 233004 (2013).
[31]B. Najjari, A. B. Voitkiv, and C. Müller, Phys. Rev. Lett. **105**, 153002 (2010).
[32]P. Piecuch, S. A. Kucharski, K. Kowalski, and M. Musiał, Comput. Phys. Commun. **149**, 71 (2002).
[33]K. Kowalski and P. Piecuch, J. Chem. Phys. **120**, 1715 (2004).
[34]P. Piecuch, J. R. Gour, and M. Włoch, Int. J. Quantum Chem. **109**, 3268 (2009).
[35]H.-J. Werner, P. J. Knowles, G. Knizia, F. R. Manby, and M. Schütz, WIREs Comput. Mol. Sci. **2**, 242 (2012).
[36]H.-J. Werner, P. J. Knowles, G. Knizia, F. R. Manby, M. Schütz *et al.*, Molpro, version 2012.1, a package of *ab initio* programs, 2012, see http://www.molpro.net.
[37]T. Korona and H.-J. Werner, J. Chem. Phys. **118**, 3006 (2003).
[38]S. M. Cybulski and R. R. Toczyłowski, J. Chem. Phys. **111**, 10520 (1999).
[39]D. Woon and J. T. H. Dunning, J. Chem. Phys. **100**, 2975 (1994).
[40]Y. Ralchenko, A. E. Kramida, J. Reader, and NIST ASD Team, *NIST Atomic Spectra Database*, version 5.0, 2012 (online).
[41]J. T. H. Dunning, J. Chem. Phys. **90**, 1007 (1989).
[42]S. Kopelke, K. Gokhberg, V. Averbukh, F. Tarantelli, and L. S. Cederbaum, J. Chem. Phys. **134**, 094107 (2011).
[43]E. Pahl, H.-D. Meyer, and L. S. Cederbaum, Z. Phys. D **38**, 215 (1996).
[44]M. Beck, A. Jäckle, G. Worth, and H.-D. Meyer, Phys. Rep. **324**, 1 (2000).
[45]E. Pahl, H.-D. Meyer, L. S. Cederbaum, D. Minelli, and F. Tarantelli, J. Chem. Phys. **105**, 9175 (1996).
[46]A. U. Hazi, J. Phys. B **16**, L29 (1983).
[47]W. Kamke, B. Kamke, H. Kiefl, and I. Hertel, Chem. Phys. Lett. **122**, 356 (1985).
[48]W. Kamke, B. Kamke, H. Kiefl, Z. Wang, and I. V. Hertel, Chem. Phys. Lett. **128**, 399 (1986).
[49]A. Golan and M. Ahmed, J. Phys. Chem. Lett. **3**, 458 (2012).
[50]K. Gokhberg, A. Trofimov, T. Sommerfeld, and L. S. Cederbaum, Europhys. Lett. **72**, 228 (2005).